Available online at www.sciencedirect.com
SCIENCE DIRECT®
Journal of Solid State Chemistry 175 (2003) 110–115
JOURNAL OF SOLID STATE CHEMISTRY
http://elsevier.com/locate/jssc

# $^{17}$O MAS NMR study of the oxygen local environments in the anionic conductors $Y_2(B_{1-x}B'_x)_2O_7$($B$, $B'$ = Sn, Ti, Zr)

Namjun Kim and Clare P. Grey*

*Department of Chemistry, State University of New York at Stony Brook, Stony Brook, NY 11794-3400, USA*

Received 16 February 2003; received in revised form 1 May 2003; accepted 12 May 2003

**Abstract**

The local environments for oxygen in yttrium-containing pyrochlores and fluorites, $Y_2(B_{1-x}B'_x)_2O_7$ ($B$ = Ti, $B'$ = Sn, Zr) are investigated by using solid state $^{17}$O MAS NMR spectroscopy. The quadrupolar coupling constants of the $I = \frac{5}{2}$ nucleus, $^{17}$O are sufficiently small for these ionic oxides, that high-resolution spectra are obtained from the MAS spectra. Different oxygen NMR resonances are observed due to local environments with differing numbers of metal cations ($Y^{3+}$, $Sn^{4+}$, $Ti^{4+}$ and $Zr^{4+}$), allowing the numbers of different local environments to be quantified and cation mixing to be investigated. Evidence for pyrochlore-like local ordering is detected for $Y_2Zr_2O_7$, which nominally adopts the fluorite structure.


*Keywords:* Solid state NMR; Oxide ionic conductor; Pyrochlore; Fluorite; $Y_2Zr_2O_7$; $Y_2Sn_2O_7$; $Y_2Ti_2O_7$

## 1. Introduction

The yttrium-containing pyrochlores ($Y_2B_2O_7$; $B$ = Sn, Ti, Zr) have been reported to show moderate anionic conductivity and thus represent potential materials for use as electrolytes in solid oxide fuel cells (SOFC) and for oxygen separation [1,2]. The Ti-containing materials also show electronic conductivity [3,4], suggesting that they may be used as electrode materials, or at the electrode–electrolyte interface. In order to improve anion conductivities in these classes of materials and lower the operating temperature of the device, or improve the power density that can be extracted from the SOFC, it is important to identify both the ions responsible for conduction, and the different oxygen local environments that do not contribute to the conduction process. We have recently shown that $^{17}$O MAS NMR methods may be used to probe oxygen-ion mobilities in anionic conductors and to identify the species responsible for conduction [5]. Here we use $^{17}$O MAS NMR methods to probe cation distributions in pyrochlore and fluorite solid solutions. The results presented in this paper demonstrate that $^{17}$O MAS NMR can be used to identify and quantify the different local environments in such solids, and how these vary for the different solid solutions $Y_2(B_{1-x}B'_x)_2O_7$($B$, $B'$ = Sn, Ti, Zr). This represents the first step towards identifying the mobile environments in these solids at higher temperatures.

While methods such as X-ray diffraction and neutron diffraction can be used to determine the long-range order in the solid, solid-state NMR spectroscopy is a sensitive probe of local structure. Despite the prevalence of oxygen in many materials of technological importance and fundamental interest, $^{17}$O solid state NMR still remains largely an under-utilized technique. In part, this is a consequence of the high cost and low natural abundance of this isotope. However, we and other workers have shown that enrichment can often be readily achieved by simply heating the oxide in $^{17}$O-enriched gas allowing a wide variety of materials to be prepared at a modest cost. $^{17}$O NMR studies of inorganic materials [6–9], such as zeolites and oxide ionic conductors have now been reported and the chemical shifts in $^{17}$O NMR have been found to be very sensitive to the oxygen local environments [10–12].

A number of oxide materials with the composition $A_2^{3+}B_2^{4+}O_7$ (e.g., $Y_2Sn_2O_7$ and $Y_2Ti_2O_7$) adopt the pyrochlore structure (Fig. 1), the $A^{3+}$ cations occupying

*Corresponding author. Fax: +1-631-632-5731.
*E-mail address:* cgrey@notes.cc.sunysb.edu (C.P. Grey).

0022-4596/03/$ - see front matter © 2003 Elsevier Inc. All rights reserved.
doi:10.1016/S0022-4596(03)00290-1

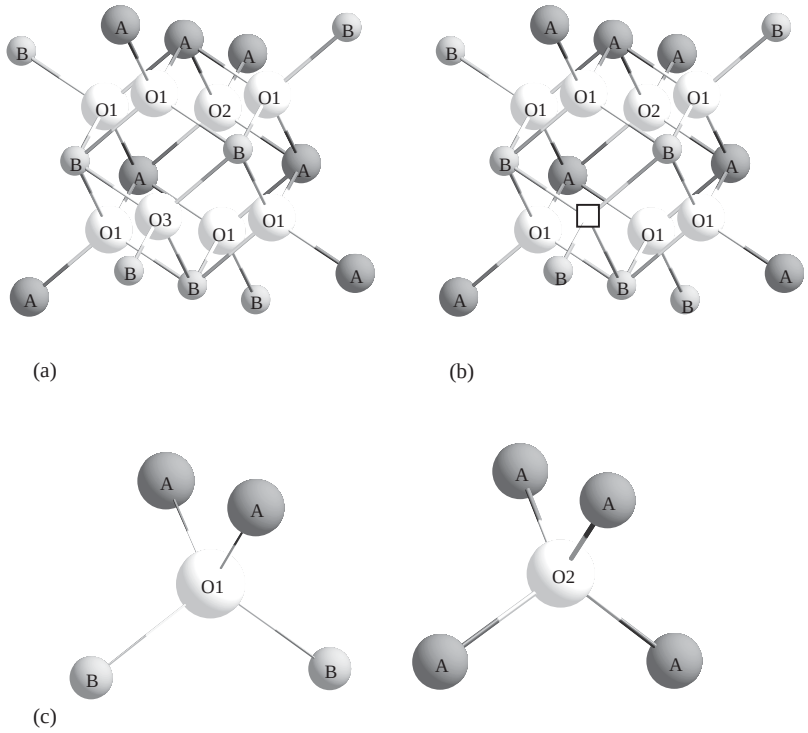


Fig. 1. The differences in oxygen local environments in the fluorite (a) and pyrochlore (b) structures. The cation-ordering in the fluorite structure has been assumed to be non-random and identical to that found in the pyrochlore structure, in order to emphasize the similarities in oxygen local environments and connectivities in the two structures. This ordering results in three different oxygen sites; the O3 site is vacant in the pyrochlore structure and is shown with a "□". The two remaining oxygen local coordination environments in the pyrochlore structure are shown in (c).

an eight-coordinate site, and the smaller $B^{4+}$ cations occupying an octahedral site [13]. As the size of the $B^{4+}$ cation approaches that of the $A^{3+}$ cation, the driving force for cation ordering on the $A$ and $B$ sites decreases and the material $Y_2^{3+}Zr_2^{4+}O_7$ adopts the fluorite structure, with complete mixing of Y and Zr on the cation sites (Fig. 1(a)) [14,15]. The fluorite and pyrochlore structures are compared in Fig. 1. The oxygen vacancy is ordered in the pyrochlore structure (on the O3 site), accounting for the typically lower conductivity of the pyrochlore vs. fluorite materials. The structures of the solid solutions with $B = Sn$ or Ti and $B' = Zr$ have been studied extensively with neutron diffraction, in order to understand the pyrochlore-to-fluorite transition and to correlate structure with conductivity in these materials [16,17]. An abrupt transition between these two phases is not observed. Although the solid solution $Y_2(Zr_xTi_{1-x})_2O_7$ adopts the pyrochlore structure for $0 \leqslant x < 0.9$, gradual occupancy of the O3 (or 8*b*) site is observed for $x > 0.3$, which is coupled with a decrease in the occupancy of the O1 (or 48*f*) site. At $x > 0.45$ cation mixing is observed on the $A$ and $B$ sites, which is correlated with a decrease in the occupancy of the O2 (8*a*) site. Complete cation mixing occurs between $0.6 < x \leqslant 0.9$. At $x \geqslant 0.9$ a disordered fluorite is observed and no evidence for preferential occupancy in the $A$ and $B$ sites was observed. Although neutron diffraction experiments are extremely sensitive to the oxygen positions and occupancies, the neutron scattering lengths for $Y^{3+}$ and $Zr^{4+}$ are similar ($b_Y = 0.775$ and $b_{Zr} = 0.716 \times 10^{-12}$ cm) [18], making it difficult to observe Y/Zr cation ordering. These ions are also isoelectronic, and so X-ray diffraction is similarly of little use. Thus, these solid solutions are re-examined by $^{17}O$ NMR in this paper, in order to probe local ordering in these materials, both in the pyrochlore and fluorite phases.

## 2. Experimental

The end members ($Y_2Sn_2O_7$, $Y_2Ti_2O_7$, and $Y_2Zr_2O_7$) and their solid solutions were prepared from $Y_2O_3$ (Aldrich 99.99%), $SnO_2$ (Fisher 99 + %), $TiO_2$ (Aldrich 99.9 + %) and $ZrO_2$ (Alfa 99.978%) by using standard ceramic methods. Stoichiometric amounts of the oxides were mixed thoroughly and heated at 1673 K for 2 days in alumina boats. All the products were characterized with a Scintag X-ray diffractometer with Cu$K\alpha$ radiation and the diffraction patterns were compared with those in the JCPDS (Joint Committee on Powder Diffraction Standards) database. The Zr-containing products were reground and calcined again at 1673 K for a further 5–10 days and 1873 K for 3 days, until single-phase products were obtained, as determined by X-ray diffraction; single-phase products were obtained

for the stannates after only one calcination step. $^{17}O$-enriched compounds were prepared by heating the samples in $^{17}O_2$ gas at 600°C for 12 h. The enriched compounds were also characterized by XRD. $^{17}O$ MAS NMR experiments were carried out at 81.4 MHz with a Bruker-600 NMR spectrometer. The spectra were obtained by using either a one pulse or Hahn echo sequence ($90° - \tau - 180° - \tau$-acquisition) with pulse widths of typically 2.0–3.0 μs ($\approx \pi/6$ pulse width), $\tau$ of one rotor period, and pulse delays of 1–5 s. Spectra were acquired with a digital filter, which prevents the satellite transitions that lie outside the selected spectral width from folding over into the region of interest and complicating the analysis of the spectra. The chemical shifts were referenced to distilled $H_2O$ (=0 ppm) as an external reference.

## 3. Results and discussion

$^{17}O$ MAS NMR spectra of the end members, $Y_2Sn_2O_7$ and $Y_2Ti_2O_7$, and one member of the solid solution [$Y_2(Sn_{0.4}Ti_{0.6})_2O_7$] are shown in Fig. 2. The end members show only two isotropic resonances, while the spectra of the solid solutions contain four distinctive resonances (165 and 385 ppm in $Y_2Sn_2O_7$ (c); 385 and 455 ppm in $Y_2Ti_2O_7$ (a); and 160, 290, 385, and 457 ppm in $Y_2(Sn_{0.4}Ti_{0.6})_2O_7$ (b)). The two oxygen sites in the pyrochlore structure (O1, O2) are surrounded by either four yttrium ions (O2; 8*a*) or two yttrium and two B ions (O1, 48*f*) (see Fig. 1(c)) [16,17]. These local environments are denoted $OY_4$ and $OY_2B_2$, respectively.

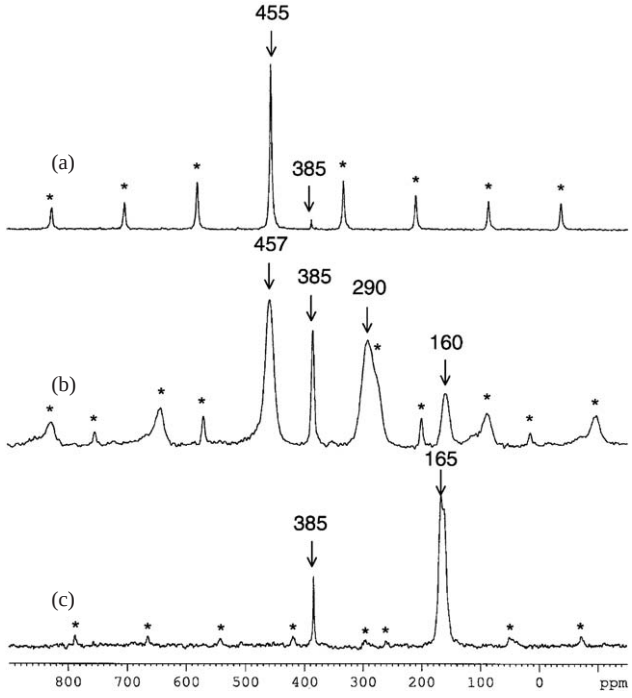


Fig. 2. $^{17}O$ MAS NMR 1-pulse spectra of (a) $Y_2Ti_2O_7$, (b) $Y_2(Sn_{0.4}Ti_{0.6})_2O_7$ and (c) $Y_2Sn_2O_7$. The spectra were acquired at 14.1 T with spinning speeds of 15 kHz. Isotropic resonances are marked with arrows. The other peaks marked with asterisks are due to the $^{17}O$ satellite transitions.

The first cation coordination shell of the O2 site is independent of the *B* cation, and the resonance at 385 ppm is assigned to this site on this basis. The more intense resonances at 165 and 455 ppm are assigned to the O1 environments, $OY_2Sn_2$ and $OY_2Ti_2$, respectively. These assignments are consistent with the relative multiplicities of the O1:O2 sites of 6:1. The assignments demonstrate that identical local environments in the two pyrochlore phases (e.g., the O2 site) give rise to resonances with very similar chemical shifts. In contrast, substitution of two Y ions for two Sn ions in the O local coordination sphere (i.e., from $OY_4$ to $OY_2Sn_2$) results in a noticeable shift of approximately –220 ppm. The resonances due to the local environments $OY_2Sn_2$ and $OY_2Ti_2$ are clearly resolved in the spectrum of the solid solution. Based on the chemical shifts of these two O1 sites, a chemical shift of approximately 310 ppm for the new local environment $OY_2SnTi$, that is likely present in the solid solution, is predicted. This is very close to the chemical shift of the additional resonance observed in this sample at 290 ppm.

The $OY_2Sn_2$ resonance of $Y_2Sn_2O_7$ is split slightly due to the second-order quadrupolar interaction, a simulation of this resonance yielding values for the quadrupole coupling constant (QCC) and asymmetry parameter of this O1 site of approximately 3 MHz and 0.4, respectively. The QCCs of the O2 site in $Y_2Sn_2O_7$ and both sites in $Y_2Ti_2O_7$ are much smaller (<1 MHz). Simulations of the sideband patterns of the spectra of $Y_2(Sn_{0.4}Ti_{0.6})_2O_7$ (spectra not shown) yielded estimates for the QCCs of the $OZY_4$ and $O1Y_2SnTi$ and $O1Y_2Ti_2$ of approximately 0.3, 3.0 and 0.7 (±0.1) MHz, respectively. A number of earlier studies have investigated the relationship between the QCC and the environments of bridging oxygen atoms in a variety of inorganic oxides [19–23], and have shown that the QCCs are sensitive to both bond distances and angles. The pyrochlore structure contains only one variable parameter *x*, which controls the position of the O1 (48*f*) oxygen position, and the coordination environments around the *A* and *B* cations. In earlier $^{119}Sn$ [24] and $^{89}Y$ MAS NMR [25] studies of these and related compounds, we showed that the chemical shift anisotropy was a sensitive measure of the site distortions at the *A* and *B* cation sites. For the tetrahedrally coordinated $O1Y_2B_2$ site, the oxygen environment becomes more distorted as *x* increases: When $x = 0$, the oxygen atom occupies the center of the tetrahedron; as *x* increases, the oxygen atom moves towards a *B*–*B* edge and the environment becomes more distorted (Fig. 3). $Y_2Sn_2O_7$ has slightly smaller *x* parameter than $Y_2Ti_2O_7$ (~0.037 vs. ~0.045, respectively), so the O1 site in $Y_2Ti_2O_7$ is slightly more

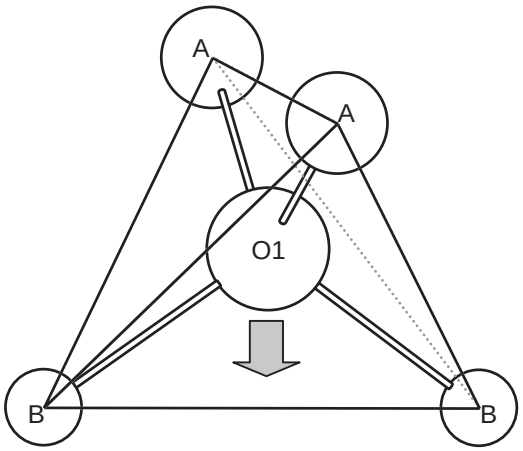


Fig. 3. The effect of the $x$-parameter on the $OA_2B_2$ local environment. The arrow represents the direction of oxygen atom movement in the tetrahedron as $x$ increases.

distorted. This is also consistent with the ionic radii of the three cations: 1.159 ($Y^{3+}$), 0.830 ($Sn^{4+}$), and 0.745 Å ($Ti^{4+}$) [26]. Thus, the small changes in coordination geometry are not dominant in controlling variations in the QCC. Instead the QCCs of these local environments, which are only slightly distorted from tetrahedral symmetry, appear to be more affected by the ionic character of the M–O bonds. Larger QCCs are seen for oxygen atoms coordinated to Sn rather than Ti, which is consistent with the differences in the Sn and Ti electronegativities.

The ratio of relative intensities of the four isotropic resonances in $Y_2(Sn_{0.4}Ti_{0.6})_2O_7$ is 0.40:0.12:0.36:0.12 for $OY_2Ti_2$:$OY_4$:$OY_2SnTi$:$OY_2Sn_2$. Differences in the QCCs of the sites will affect the intensities of the isotropic resonances somewhat so that the intensity of the isotropic resonance is not necessarily directly proportional to the concentration of the local environment in the solid [27]. The intensities can be readily corrected by using the graphical method of Massiot et al. or by simulation [27,28]. Simulations of our spectra [28] indicate that for sites with QCCs of $>1$ MHz, the corrections are minimal for the conditions used to acquire the spectra, but can be large for sites with small QCCs ($=0.3$ MHz). Corrected intensities of 0.38:0.09:0.40:0.13 ($OY_2Ti_2$:$OY_4$:$OY_2SnTi$:$OY_2Sn_2$), are estimated, which are in reasonable agreement with the intensity ratio predicted by assuming a random distribution of Sn and Ti cations on the $B$ sites (0.31:0.14:0.41:0.14).

Fig. 4 shows the $^{17}O$ NMR spectra of three members of the $Y_2(Zr_xTi_{1-x})_2O_7$ series ($x=1$, 0.8, and 0.3). Based on the earlier neutron diffraction study, the $x=0.3$ and 0.8 members of the solid solution adopt a disordered pyrochlore structure, while $Y_2Zr_2O_7$ adopts a fluorite structure [16]. A noticeable increase in the line width of the resonances is observed in comparison

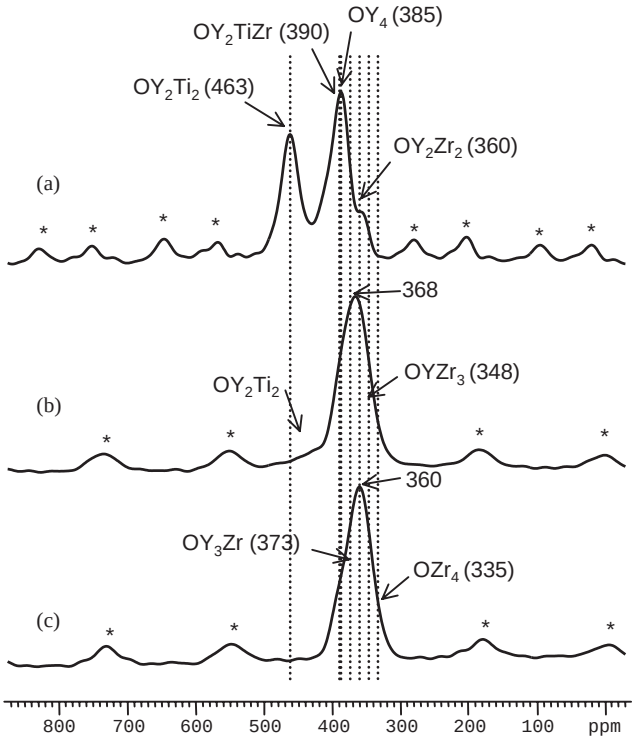


Fig. 4. $^{17}O$ MAS NMR spectra of (a) $Y_2(Zr_{0.3}Ti_{0.7})_2O_7$, (b) $Y_2(Zr_{0.8}Ti_{0.2})_2O_7$ and (c) $Y_2Zr_2O_7$. The spectra were acquired with Hahn echo pulse at 14.1 T with spinning speeds of 15 kHz. Isotropic resonances are marked with arrows and sidebands are marked with asterisks. Dashed lines indicate positions for the different local environments. In the case of the $OZr_xY_{4-x}$ environments with $x=1$, 3, and 4, these are estimated based on the shifts of the $x=0$ and 2 environments.

to the line widths observed for the Sn/Ti series. $^{17}O$ NMR experiments performed at lower field strengths demonstrated that the source of the broadening in these spectra arises from a distribution in chemical shifts due to structural disorder, rather than from the second-order quadrupolar interaction (caused by large $^{17}O$ QCCs). Furthermore, $Zr^{4+}$–O bonds are expected to be more ionic than $Sn^{4+}$–O bonds and thus smaller QCCs for Zr-containing local environments are expected. This indicates that the Y–Zr–Ti pyrochlores are more disordered than the Y–Sn–Ti pyrochlores, which is consistent with their higher conductivities [17].

Despite the increase in the breadth of the resonances, four individual resonances can still be resolved in the spectrum of $Y_2(Zr_{0.3}Ti_{0.7})_2O_7$. Based on the assignments of the spectra of the Y–Sn–Ti pyrochlores, the resonances at 463 and 385 ppm are assigned to $O1Ti_2Y_2$ and $O2Y_4$ sites, respectively. The resonance at 360 ppm is assigned to $O1Zr_2Y_2$, since this resonance dominates the spectra of $Y_2(Zr_{0.8}Ti_{0.2})_2O_7$ and $Y_2Zr_2O_7$, where this is expected to be the most common local environment. Thus, the resonance at 390 ppm must be due to $O1Y_2TiZr$. The $^{17}O$ NMR spectrum of $Y_2(Zr_{0.8}Ti_{0.2})_2O_7$, which shows a decrease in the

intensity of the resonances assigned to O1 sites coordinated to titanium and an increase in the intensity of the resonances due to O1 coordinated to zirconium, is consistent with these assignments. Previous NMR studies of monoclinic $ZrO_2$ reported two $^{17}O$ resonances at 401 and 324 ppm, which were assigned, based on a relationship between the chemical shift and coordination number, to three coordinated and four coordinated oxygen environments, respectively [11]. This is in good agreement with the estimate of the chemical shift of the $OZr_4$ local environment of 335 ppm, calculated from the chemical shifts of $OY_4$ (385 ppm) and $OY_2Zr_2$ (360 ppm) by assuming that the shifts depend linearly on the number of Y and Zr atoms in the oxygen local environment, further validating our assignments.

The observation of four distinct sites in $Y_2(Zr_{0.3}Ti_{0.7})_2O_7$ is consistent with the neutron diffraction study where this material was shown to adopt the pyrochlore structure with no $A/B$ mixing. Relative intensities for the four sites, predicted based on random mixing of Ti and Zr on the $B$ site (Table 1), are close to the relative intensities estimated by deconvolution of the spectra, indicating that the ordering is essentially that of the pyrochlore structure. The resonances of $Y_2(Zr_{0.8}Ti_{0.2})_2O_7$ are much broader and it is very difficult to separate the contributions from the different local environments that give rise to the resonance at around 368 ppm. The relative intensities of the four resonances, predicted by assuming a pyrochlore structure with random mixing on the $B$ site, but no $A/B$ cation mixing are again shown in Table 1. The local environment $OY_2Zr_2$ is the most abundant, consistent with the experimental spectra. The resonances due to $OY_2TiZr$ and $OY_4$ are, however, present in lower concentrations than expected based on Table 1. Furthermore, the resonance due to $OY_2Zr_2$ is extremely broad, and intensity is present in the chemical shift range predicted for the local environment $OYZr_3$ (approximately 348 ppm, based on the shifts of $OY_4$ and $OY_2Zr_2$ for $Y_2(Zr_{0.3}Ti_{0.7})_2O_7$). This local environment can only result if cation mixing between the $A$ and $B$ sites has occurred, creating new environments for O such as $OY_xB_{4-x}$, where $x = 1$ or 3 [16].

The spectrum of $Y_2Zr_2O_7$ is asymmetric, and a shoulder to higher frequencies of the main resonance at 361 ppm is clearly observed. $Y_2Zr_2O_7$ adopts the fluorite structure, with, in principle, complete random mixing of the cations in all the sites and partial occupancy (0.875) of all the O sites. This results in five different local environments for O: $OA_4$, $OA_3B$, $OA_2B_2$, $OAB_3$, and $OB_4$. The relative intensities of these environments can again be readily calculated (Table 1); their estimated chemical shifts are shown in Fig. 4 and in Table 1. This model predicts a symmetric distribution of resonances about the $OA_2B_2$ resonance, which is not consistent with experiment. Simulation of the experimental spectrum, using the predicted chemical shifts of the five environments as constraints yields approximate intensities of 13:20:46:14:6 for the $OY_4$:$OY_3Zr$:$OY_2Zr_2$:$OYZr_3$:$OZr_4$ (again the data have been corrected for the smaller QCC of the $OY_4$ environment; QCCs of the other environments are between 1 and 1.5 MHz). The probabilities of the different local environments were then calculated for different models. The two extreme models which (1) assume complete mixing of the $A$ and $B$ cations, but allow for no, or partial, occupancy of the O3 site (of the original pyrochlore structure), or (2) assume equal occupancy of the all the oxygen sites, but allow for some cation ordering in the $A$ and $B$ sites, both result in symmetric $^{17}O$ NMR lineshapes centered around the $OY_2Zr_2$ resonance and thus cannot explain the experimental data (N.b., model (2), but with no cation mixing, can be immediately ruled out as only three local environments, $OY_4$, $OZr_2Y_2$ and $OZr_4$ are created (see Table 1)). An asymmetric lineshape can only result when oxygen occupancy is non-random, but instead is correlated with the nature of the specific local environment, in either of these models.

Table 1
Calculated concentrations (%) and the experimental or predicted ($OZrY_3$ and $OY_4$) shifts of the different local environments in the solid solution $Y_2(Zr_xTi_{1-x})_2O_7$, as a function of $x$. For $x = 1$, four different structural models have been considered

| $x$ | 0.3[a] | 0.8 | 1 | | | | Chemical shift (ppm) |
|---|---|---|---|---|---|---|---|
| | | | Pyrochlore | Fluorite | Anion ordering[b] | Cation ordering[c] | |
| $OY_2Ti_2$ | 42.0 (38) | 3.4 | | | | | 463 |
| $OY_2TiZr$ | 36.0 (44) | 27.4 | | | | | 390 |
| $OZr_4$ | | | | 6.25 | 6.25 | 12.5 | 335 |
| $OZr_3Y$ | | | | 25.0 | 25.0 | | 348 |
| $OZr_2Y_2$ | 7.7 (9) | 54.8 | 85.7 | 37.5 | 37.5 | 75.0 | 360 |
| $OZrY_3$ | | | | 25.0 | 25.0 | | 373 |
| $OY_4$ | 14.3 (9) | 14.3 | 14.3 | 6.25 | 6.25 | 12.5 | 385 |

[a] Experimental values in parentheses; these values have been corrected to take into account the QCCs of the different oxygen sites, which are similar (0.7–1.5 MHz) for all the sites except the $OY_4$ local environment (0.3 MHz).
[b] 0% occupancy of O3 sites and complete cation mixing are assumed.
[c] No mixing between the $A$ and $B$ cation sites and random occupancy of all three oxygen sites are assumed.

I.e., in order to produce the experimentally observed lineshape, the occupancies for O in local environments such as $OZr_4$ and $OYZr_3$ are considerably lower than predicted based on either model. Thus, a combination of both cation mixing and anion ordering is required to produce the experimentally observed spectrum. This conclusion indicates that there is some remaining pyrochlore-like ordering and is somewhat different from the previous neutron diffraction study [16], where the structure of the $x = 0.9$ sample was refined as an oxygen deficient fluorite, with complete $A/B$ mixing. Note that we cannot completely exclude the possibility that some of these differences arise from differences in sample preparation methods. The study is in agreement with selected area electron diffraction (SAED) studies [29], where micro-domains with pyrochlore-like ordering and with C–$Ln_2O_3$ were detected.

## 4. Conclusion

This report shows that chemical shift of solid state $^{17}O$ NMR is very sensitive to the nature of the transition metal atoms coordinated to the central oxygen atom in a series of tetrahedrally coordinated oxygen environments. In the systems investigated here, where the long-range structures of the materials are similar, the chemical shifts obtained for each local environment $OX_{4-y-z}Y_yZ_z$ can be predicted with reasonable accuracy by summing the contributions from each O–X/Y/Z bond to the total shift. For example, the chemical shift of the local environment $OY_2SnTi$ may be estimated based on the shifts for the $OY_2Sn_2$ and $OY_2Ti_2$ local environments. The $^{17}O$ QCC is sensitive to the ionic character of the M–O bonds; small QCCs were obtained for the more ionic materials, while larger QCCs were observed for the more covalent local environment $OY_2Sn_2$.

The intensities (and thus concentrations) of the different local environments were used to characterize local ordering (cation and anion) in these materials and the disordering associated with the pyrochlore to fluorite transition. The results for $Y_2Zr_2O_7$ which nominally adopts the fluorite structure, indicated that (i) cation mixing between the $A$ and $B$ (pyrochlore) sites is not complete and (ii) the occupancy of the O3 site is intermediate between that expected for the pyrochlore (0) and fluorite (0.875) structures. An analysis of a wider range of compositions in the $Y_2(Ti_{1-x}Zr_x)_2O_7$ solid solution, prepared by a variety of synthetic routes, is currently underway in order to probe ordering in greater detail. Finally, $^{17}O$ MAS NMR spectroscopy is expected to be particularly useful for characterizing materials that contain cations with similar X-ray and neutron scattering factors.

## References


[1] J.C. Boivin, G. Mairesse, Chem. Mater. 10 (1998) 2870.
[2] K.R. Kendall, C. Navas, J.K. Thomas, H.-C.Z. Loye, Solid State ionics 82 (1995) 215.
[3] S.S. Liou, W.L. Worrel, Appl. Phys. A 49 (1989) 25.
[4] S. Kramer, M. Spears, H.L. Tuller, Solid State Ionics 72 (1994) 55.
[5] N. Kim, C.P. Grey, Science 297 (2002) 1317.
[6] S. Adler, J.A. Reimer, Solid State Ionics 91 (1996) 175.
[7] E. Oldfield, C. Coretsopoulos, S. Yang, L. Reven, H.C. Lee, J. Shore, O.H. Han, E. Ramli, D. Hinks, Phys. Rev. B 40 (1989) 6832.
[8] M.E. Smith, H.J. Whitfield, J. Chem. Soc. Chem. Comm. (1994) 723.
[9] Z. Xu, H. Maekawa, J.V. Oglesby, J.F. Stebbins, J. Am. Chem. Soc. 120 (1998) 9894.
[10] G.L. Turner, S.E. Chung, E. Oldfield, J. Magn. Reson. 64 (1985) 316.
[11] T.J. Bastow, S.N. Stuart, Chem. Phys. 143 (1990) 459.
[12] T.J. Bastow, P.J. Dirken, M.E. Smith, H.J. Whitfield, J. Phys. Chem. 100 (1996) 18539.
[13] M.A. Subramanian, G. Aravamudan, G.V.S. Rao, Prog. Solid State Chem. 15 (1983) 55.
[14] A.W. Sleight, Inorg. Chem. 8 (1969) 1807.
[15] K.E. Sickafus, L. Minervini, R.W. Grimes, J.A. Valdez, M. Ishimaru, F. Li, K.J. McClellan, T. Hartmann, Science 289 (2000) 748.
[16] C. Heremans, B.J. Wuensch, J. Solid State Chem. 117 (1995) 108.
[17] B.J. Wuensch, K.W. Eberman, C. Heremans, E.M. Ku, P. Onnerud, E.M.E. Yeo, S.M. Haile, J.K. Stalick, J.D. Jorgensen, Solid State Ionics 129 (2001) 111.
[18] V.F. Sears, Neutron News 3 (1992) 29.
[19] S. Schramm, E. Oldfield, J. Am. Chem. Soc. 106 (1984) 2502.
[20] H.K.C. Timken, S.E. Schramm, R.J. Kirkpatrick, E. Oldfield, J. Phys. Chem. 91 (1987) 1054.
[21] P.J. Grandinetti, J.H. Baltisberger, I. Farnan, J.F. Stebbins, U. Werner, A. Pines, J. Phys. Chem. 99 (1995) 12341.
[22] T.M. Clark, P.J. Grandinetti, Solid State NMR 16 (2000) 55.
[23] L.M. Bull, B. Bussemer, T. Anupold, A. Reinhold, A. Samoson, J. Sauer, A.K. Cheetham, R. Dupree, J. Am. Chem. Soc. 122 (2000) 4948.
[24] C.P. Grey, C.M. Dobson, A.K. Cheetham, R.J.B. Jakeman, J. Am. Chem. Soc. 111 (1989) 505.
[25] C.P. Grey, M.E. Smith, A.K. Cheetham, C.M. Dobson, R. Dupree, J. Am. Chem. Soc. 112 (1990) 4670.
[26] R.D. Shannon, Acta Crystallogr. A32 (1976) 751.
[27] D. Massiot, C. Bessada, J.P. Coutures, F. Taulelle, J. Magn. Reson. 90 (1990) 231.
[28] J.P. Amoureux, C. Ferandez, P. Granger, in: P. Granger, R.K. Harris (Eds.), Multinuclear Magnetic Resonance in Liquids and Solids-Chemical applications, Kluwer Academic, Netherlands, 1990, p. 409.
[29] J.T.S. Irvine, A.J. Feighery, D.P. Fagg, S. Garcia-Martin, Solid State Ionics 136–137 (2000) 879.